Electronic spectral diffusion in glasses: The influence of coupling to the medium on experimental observables

David Zimdars and M. D. Fayer
Department of Chemistry, Stanford University, Stanford, California 94305

(Received 3 November 1995; accepted 29 November 1995)

The theory of electronic dephasing in low temperature glasses is extended to include the possibility that the strength of coupling of the chromophore to the solvent medium depends on the nature of the bath dynamical processes and the nature of the chromophore and, therefore, the chromophore-bath coupling can vary as a function of the rate of the dynamics of the medium. In the context of the sudden jump two-level system (TLS) model of low temperature glasses, this theory is used to reconcile the apparent contradiction implied by differences observed in spectral diffusion data for cresyl violet and metal-porphyrins in deuterated ethanol glass at 1.5 K. Previously, the coupling strength of a chromophore to the TLS has been assumed to be independent of rate of the transition between TLS states. Within the context of this approximation, spectral diffusion data yield, $P_i(R)$, the intrinsic TLS fluctuation rate distribution. With the inclusion of the rate dependent coupling, $C(R)$, it is shown that the spectral diffusion observables actually yield $P_i(R)C(R)$. Therefore, the observed lack of spectral diffusion for a particular chromophore over some range of times can imply $C(R)$ is zero rather than the current interpretation that $P_i(R)$ is zero. To illustrate the importance of $C(R)$, a hueristic model is analyzed. A fluctuation rate distribution is introduced that consists of the sum of three log-normal functions each associated with a specific class of dynamics occurring over three overlapping ranges of rates. The uncharged and nonpolar metal porphyrins is taken to couple to TLS strain dipoles, while the charged and polar cresyl violet also couples to TLS electric dipoles. By taking one of the types of TLS dynamics to only give rise to electric dipole fluctuations, it is possible to fit all of the experimental data in deuterated ethanol with a single intrinsic distribution of TLS fluctuation rates. This analysis of previously reported data is supported by the presentation of new stimulated photon echo data on both cresyl violet and zinc meso-tetraphenyl porphine in deuterated ethanol. [S0021-9606(96)00510-3]

I. INTRODUCTION

Amorphous solids at low temperature exhibit markedly different physical and thermal properties than their crystalline counterparts.[1] Many important natural and artificial materials, such as polymeric solids, are glasses. In spite of their importance, the understanding of the microscopic behavior of glasses continues to be an important, unsolved problem in chemistry, physics, and materials science.[2,3] The lack of long range translational symmetry makes the theoretical description of dynamics in glassy solids a difficult task. Because of their complexity, experiments which adequately characterize crystals (heat capacity measurements, scattering experiments, etc.) do not provide enough information to uniquely determine the nature of glass dynamics. Therefore a very wide variety of techniques, including time-resolved optical spectroscopy, have been used to extend the base of knowledge of low temperature glasses.

The electronic absorption spectra of chromophores dissolved in solid matrices generally show inhomogeneously broadened transitions. In amorphous solids such as organic glasses below 4 K, the inhomogeneous linewidth is many orders of magnitude greater than the homogeneous linewidth. Various line narrowing techniques have been used to extract an underlying homogeneous linewidth. The homogeneous linewidth (and lineshape) contains information on the microscopic dynamics of the solvent that perturbs the optical transition of the dissolved chromophore. Examples of experimental techniques that extract a narrowed linewidth from under the inhomogeneous absorption line are the two pulse photon echo, three pulse stimulated photon echo, and optical hole burning (HB).[4–9] Each of these techniques is sensitive to perturbations which induce optical dephasing on a characteristic time scale T_w.[10–14] T_w is the ''waiting time'' for each experiment. In a hole burning experiment, it is the time between writing and reading the hole. In a stimulated photon echo, it is the time between the second and third pulses in the pulse sequence. The two pulse echo experiment corresponds to $T_w=0$, and yields the minimum observable homogeneous linewidth. As T_w is increased (stimulated echo or hole burning experiment), the observed ''homogeneous'' linewidth may increase. The processes which increase the linewidth beyond the homogeneous width measured by the two pulse echo are referred to as spectral diffusion. Characterizing spectral diffusion yields information on the microscopic dynamics of the solvent and the influence of solvent dynamics on the chromophore.

In a simple crystal, electronic dephasing is induced by fast phonon fluctuations about an equilibrium crystal structure. The fluction rate-distribution can be calculated from the

Debye density of states that describes acoustic phonons.[15,16] Other dynamical processes, such as nuclear spin flips, can also cause optical dephasing.[10,14] Again, the structure and chemical composition of the crystal can provide the necessary information to describe observations of optical dephasing.[14]

In contrast, glasses are disordered, non-equilibrium systems. The structure of glasses can evolve on timescales from picoseconds to possibly hundred of years.[17–19] At very low temperatures, the phonon dynamics are not directly responsible for optical dephasing in glasses.[20] The phonon bath assists in altering the metastable structure of the glass about the dissolved chromophores. These structural changes can alter the electric and magnetic moments and the mechanical properties of the host glass which perturb the optical transitions, and thereby induce optical dephasing.

Theoretical treatments of optical dephasing in glasses have assumed that the influence of the structural evolution on the chromophore can be decomposed into the combined action of a distribution of localized perturbing centers.[21–24] The perturbing centers are taken to be uncorrelated on a time scale much greater than that of the experiment. There is no *a priori* knowledge of the fluctuation rate distribution of these perturbers or the coupling strength of the various perturbers to the chromophore. In fact, the precise physical nature of the perturbers themselves is not known. However, for low temperature glasses, these perturbers are often modeled as a bath of tunneling two-level systems (TLS). The TLS model was proposed to account for the observed temperature dependence of the specific heat and thermal conductivity of glasses by Anderson *et al.*[25] and, independently, by Phillips.[26] The TLS model has been used to describe electronic dephasing in low temperature organic glasses by several workers.[12,23,24,27,28] The time-scale dependence of optical dephasing due to spectral diffusion was described theoretically by Bai and Fayer for TLS (Ref. 13) and later more generally (Ref. 14). The existence of TLS coupled to the chromophore, which have a very broad distribution of tunneling rates, will lead to the observation of spectral diffusion.

The contribution of spectral diffusion to electronic dephasing as a function of T_w can be used to classify the dynamical processes active in the system. It was shown by Bai and Fayer[14] that experimental techniques where the waiting time T_w can be varied continuously can be used to map out a distribution of rates, $P(R)$, called the fluctuation rate distribution. For the TLS model of low temperature glasses, this distribution of rates maps out the probability of finding a TLS perturber with a relaxation rate R. At low temperatures, where the bath of TLS dominates the heat capacity, $P(R)$ is directly related to these dominate modes of the heat bath.

As discussed by Bai and Fayer[14] in contrast to the coupling strength, which is determined by both the optical center and the nature of the perturbers, the fluctuation rate distribution $P(R)$ is an *intrinsic* property of the perturbers, and hence an *intrinsic* property of the host sample. Bai and Fayer[14] derived a general relation between a T_w dependent dephasing measurement and the fluctuation rate distribution,

$$\frac{\partial \ln[I_s(T_w)]}{\partial T_w} \propto -\int dR P(R) \exp(-RT_w). \tag{1.1}$$

$I_s(T_w)$ is the echo decay function, and here $P(R)$ is the rate distribution on a logarithmic time scale. This states that the derivative of the echo-decay function is directly proportional to the Laplace transform of the fluctuation rate distribution. In the derivation of Eq. (1.1), the coupling of the perturbers (TLS) to the chromophore is a function of distance. However, the coupling was assumed to be independent of fluctuation rate, R. Thus, two TLS equidistant from a chromophore, one undergoing fast transitions and the other undergoing slow transition, were assumed to have the same coupling strength to the optical center. It is possible that TLS dynamics occurring on vastly differing time scales arise from distinct physical process, e.g., translation or rotation. Different TLS physical processes can give rise to different magnitudes of the perturbation of the optical center. Therefore, it is important to consider the consequences of no longer assuming that the TLS coupling strength to the optical center is independent of the fluctuation rate, R.

If the coupling to the optical center is not independent of R, the spectral diffusion experimental observables will reflect the fluctuations scaled by the strength of the coupling. If some TLS dynamics have zero coupling, the measured $P(R)$ will not reflect these dynamics at all. Unless all types of TLS are coupled to the optical center equally, the measured $P(R)$ will not reflect the intrinsic $P(R)$. Therefore it is useful to make the notational distinction between the distribution of rates intrinsic to the glass, $P_i(R)$, and the distribution of rates modified by the coupling strength that actually causes electronic dephasing, $P_c(R)$. $P_c(R)$ is measured in an experiment. Equation (1.1) is based on the assumption that $P_c(R)=P_i(R)$. Experimental evidence shows that TLS couple to chromophores through a dipolar interaction, i.e., the coupling strength is $\propto 1/r^3$. The interaction can arise from electric or elastic strain dipolar coupling. If all perturbers with rate R have a coupling strength proportional to C/r^3, different ranges of rates may have different constants of proportionality C. Furthermore, the magnitudes of the constants C and the variation with R can depend on the chromophore used as a probe. Different chromophores may be coupled more or less strongly to different portions of $P_i(R)$.

As will be developed in detail in Sec. II, to account for differences in coupling for processes with different rates, a rate dependent coupling constant, $C(R)$, is introduced. The coupled (observed) rate distribution function is related to the intrinsic rate distribution by

$$P_c(R)=C(R)P_i(R). \tag{1.2}$$

Thus, for a glass possessing some $P_i(R)$, two different chromophores can yield different distribution functions $P_c(R)$ if their coupling functions, $C(R)$, differ. Whenever the observed $P_c(R)\neq 0$, it implies that both $P_i(R)\neq 0$ and $C(R)\neq 0$. If for some *other* chromophore it is seen that for some range of R, $P_c(R)=0$, then it can be reasonably assumed that $C(R)=0$ for that chromophore since $P_i(R)$ is unchanged.

There are experiments that show that different chromophores yield different $P_c(R)$ in the same glassy host. Fast spectral hole-burning measurements performed by Littau and Fayer[29] on the cationic dye cresyl violet (CV) in phase I ethanol-*d* glass at 1.5 K showed that $P_c(R) \propto 1/R$ over the limits 10^1 Hz$<R<10^5$ Hz. However, stimulated photon echo measurements performed by Meijers and Wiersma[30–32] on the neutral chromophore magnesium porphine (MgP) in the same solvent at the same temperature suggested no glass dynamics occur over the range of rates 10^3 Hz to 10^6 Hz. These two sets of experiments conflict in the region 10^3 Hz$<R<10^5$ Hz where the CV data show $P_c(R) \propto 1/R$ while the MgP data show $P_c(R)=0$, indicating a rate dependent difference in the coupling of the two chromophores to the same bath of perturbers. These results will be discussed in detail in Sec. III using the theory developed in Sec. II. In Sec. IV, new short T_w stimulated photon echo data on zinc meso-tetra phenyl porphine and cresyl violet in glassy ethanol are presented. These data are also shown to be consistent with rate dependent coupling to the TLS.

II. THE STIMULATED PHOTON ECHO AND HOLE BURNING WITH RATE DEPENDENT COUPLING

A. General formulation

In this section, the theory of Bai and Fayer[14] is extended to include a rate dependent coupling between the TLS and the chromophore in the calculation of the stimulated photon echo and hole burning observables. For a stimulated photon echo experiment, where τ is the delay between the first and second pulses, and T_w is the delay between the second and third pulse, the decay of the echo signal due to the time-varying modulation of the transition frequency by the perturbation bath is governed by the four-time correlation function (specified by the three time intervals):[12–14,33]

$$C(\tau,T_w,\tau)=\left\langle \exp\left(i\sum_j^N \varphi_j(\tau,T_w)\right)\right\rangle_{H,\mathbf{r},\lambda} \tag{2.1}$$

and

$$\varphi_j(\tau,T_w)=\int_0^{\tau}\Delta\omega_j(t)dt-\int_{T_w+\tau}^{T_w+2\tau}\Delta\omega_j(t)dt, \tag{2.2}$$

where N is the number of discrete perturbers in the averaging volume V. H denotes the average over the time-varying path history of the perturbation $\Delta\omega_j(t)$. The functional form of $\Delta\omega_j(t)$ is determined by the nature of the perturbers for the particular glass-chromophore system. $\mathbf{r}$ denotes the average over the spatial distribution of TLS coupled to the chromophores and λ denotes the average over the internal parameters of the TLS. A hole burning experiment is described by the Fourier transform of the same four time correlation function.[12] Thus hole burning is equivalent to a frequency domain stimulated echo experiment. In a hole burning experiment, T_w is the time between burning and reading the hole.

If the time-varying frequency modulation $\Delta\omega_j(t)$ originates from the sudden jumps of a TLS perturber "j" between the two levels of its potential, the phase perturbation due to this perturber can be written as

$$\varphi_j(\tau,T_w)=\Delta\omega_j\left(\int_0^{\tau}h_j(t)dt-\int_{T_w+\tau}^{T_w+2\tau}h_j(t)dt\right), \tag{2.3}$$

where $h(t)$ is a random telegraph function that varies with time, having values of either $+1$ or -1.[22] $\Delta\omega_j$ represents the strength of the coupling of the TLS perturber to the electronic transition. In general, the coupling strength will depend on the distance $\mathbf{r}$ from the chromophore to the jth perturber. The TLS are assumed to be very weakly coupled to each other, and therefore to be statistically independent. It is also assumed that each chromophore feels the effects of a large number of TLS, so that $N \gg 1$. The correlation function is, then,

$$C(\tau,T_w,\tau)=\exp\{-N\langle 1-\exp[i\varphi(\tau,T_w)]\rangle_{H,\mathbf{r},\lambda}\}. \tag{2.4}$$

The dynamic behavior of each tunneling TLS is determined by two internal parameters: the energy separation between the two levels, E, and the coupling of the TLS to the heat bath. The action of the heat bath on the TLS causes the sudden jumps between the two levels, which in turn induces the optical dephasing of the chromophore. The coupling of the TLS to the heat bath can be modeled by the phenomenological parameter R, the relaxation rate between the two levels towards thermal equilibrium. Following Ref. 14 the history average is performed first. Using the results in Refs. 14 and 22, performing the history average gives

$$\langle 1-\exp(i\varphi)\rangle_H=F_1(R\tau,\Delta\omega;x)+F_2(R\tau,\Delta\omega;x)\times[1-\exp(-RT_w)], \tag{2.5}$$

where $x=E/2kT$. F_1 and F_2 are integrals over modified Bessel functions. For $T_w=0$, the first term of this equation, F_1, describes the dephasing of the two-pulse echo, and the second term is zero. If perturbers exist with $R \approx 1/\tau$ then there is a contribution to the homogeneous dephasing from the TLS bath. F_1 gives the minimum pure dephasing linewidth (Fourier transform of the photon echo decay). The second term on the right-hand side of Eq. (2.5) describes the additional dephasing introduced during the finite waiting time, T_w, in the stimulated photon echo or hole burning experiment. This waiting time-dependent term contains the contribution to the linewidth from spectral diffusion. The function F_2 is independent of T_w and determines only the functional form of the stimulated photon echo decay arising from spectral diffusion (line shape in hole burning experiments). The stimulated echo decay rate (linewidth) as a function of T_w is determined by the factor $1-\exp(-RT_w)$, the distribution of relaxation rates $P(\mathbf{r},E,R)$, and chromophore coupling coefficient $\Delta\omega$.

Evaluation of the average of Eq. (2.5) when $\tau \approx T_w$ cannot be done analytically[34] and must be evaluated numerically. However, when $T_w \gg \tau$, Eq. (2.5) can be evaluated analytically:[14]

$$\langle 1-\exp(i\varphi)\rangle_H = \sin^2(\Delta\omega\tau)\mathrm{sech}^2(x)[1-\exp(-RT_w)]. \tag{2.6}$$

Equation (2.6) implies

$$F_2(R\tau,\Delta\omega;x) = \sin^2(\Delta\omega\tau)\mathrm{sech}^2(x), \quad \tau \ll T_w, 1/R. \tag{2.7}$$

Equation (2.7) is accurate when $T_w \geqslant 10\tau$. In practice, this describes the T_w dependent dephasing over many decades of time since the decay of the two-pulse echo at low temperature is on the order of 100 ps while T_w can be varied up to tens of milliseconds for stimulated photon echoes and hours for hole burning.

With the history average H performed, the four-time correlation function in the long T_w limit is

$$C(\tau,T_w,\tau) = \exp\{-N\langle \sin^2(\Delta\omega\tau)\mathrm{sech}^2(E/2kT) \times[1-\exp(-RT_w)]\rangle_{\mathbf{r},E,R}\}. \tag{2.8}$$

The averages over $\mathbf{r}$, E, and R remain. The average over $\mathbf{r}$, E, and R in Eq. (2.8) can be written as

$$= \int d\mathbf{r}\, dE\, dR P(\mathbf{r},E,R)\sin^2(\Delta\omega\tau)\mathrm{sech}^2(E/2kT) \times[1-\exp(-RT_w)]. \tag{2.9}$$

In Eq. (2.9), $P(\mathbf{r},E,R)$ is a probability distribution function that describes the probability of finding a TLS perturber at distance and orientation $\mathbf{r}$, with energy splitting E and relaxation rate R.

As long as the back interaction of the optical center on the TLS is weak compared with that of the heat bath coupled to the perturbers, $P(\mathbf{r},E,R)$ is a distribution function that describes properties intrinsic to the perturbers and, hence, describes properties intrinsic to the solvent. The absence of back coupling also implies that the internal parameters, E and R are independent of $\mathbf{r}$. In glasses, it is reasonable to assume that the perturbers are uniformly distributed over all space, i.e., E and R are not dependent on position. In this case the distribution function $P(\mathbf{r},E,R)$ may be factored and

$$P(\mathbf{r},E,R) = P(E,R)P(\mathbf{r}). \tag{2.10}$$

Then Eq. (2.9) becomes

$$\propto \int dR\, dE\, P(E,R)\mathrm{sech}^2(E/2kT) \times[1-\exp(-RT_w)]\int d\mathbf{r}\, P(\mathbf{r})\sin^2(\Delta\omega\tau). \tag{2.11}$$

Experimental evidence indicates that the coupling of TLS to a chromophore is via a dipolar interaction.[12,23,35,36] Then for electric or strain dipolar coupling, the coupling coefficient, $\Delta\omega$, will fall off as $1/r^3$,[12,36] i.e.,

$$\Delta\omega(\mathbf{r},R) \propto \frac{\eta C(R)}{r^3}. \tag{2.12}$$

$C(R)$ is the coupling constant of the TLS to the chromophore for the rate R. Since $C(R)$ may depend on the rate R, the coupling coefficient is written as $\Delta\omega(\mathbf{r},R)$. In the previous theoretical development, the coupling coefficient was taken to be independent of R. As shown later, the possibility that the coupling depends on the TLS rate has important ramifications. The parameter η is the angular part of the dipolar coupling. The average over $\mathbf{r}$ in Eq. (2.11) is proportional to

$$\int d\mathbf{r}\, P(r)\sin^2\left(\frac{\eta C(R)}{r^3}\,\tau\right). \tag{2.13}$$

This average has been performed previously[13,14] and yields,

$$\int d\mathbf{r}\, P(r)\sin^2\left(\frac{\eta C(R)}{r^3}\,\tau\right) = \frac{2\pi^2\bar{\eta}C(R)}{3V}\,\tau, \tag{2.14}$$

where $\bar{\eta}$ is a constant resulting from the angle average.

Before completing the remaining averages over energy and rate, we note that the four time correlation function is now of the form

$$C(\tau,T_w,\tau) = \exp\left(-\frac{2\pi^2 N\bar{\eta}}{3V}\,\tau\langle C(R)\mathrm{sech}^2(E/2kT)[1-\exp(-RT_w)]\rangle_{E,R}\right). \tag{2.15}$$

N is the number of TLS in the averaging volume V. Therefore, N/V is the number density of TLS. Equation (2.15) shows that the stimulated echo decay, as a function of τ at fixed T_w, is exponential in the long waiting time limit $T_w \gg \tau$, and that the hole-burning line shape is Lorentzian.

The average over energy E is the same as that in Bai and Fayer.[14] The ensemble average over E and R in Eq. (2.15) can be rewritten as

$$\propto \int dR\Omega(R)[1-\exp(-RT_w)] \times \int dE P(E,R)\mathrm{sec}\, h^2(E/2kT). \tag{2.16}$$

In Eq. (2.16) the functions $1-\exp(-RT_w)$ and $\mathrm{sech}^2(E/2kT)$ act as cutoffs, restricting the observed opti-

cal dephasing to only those perturbers with $E \lesssim 2kT$ and $R \lesssim 1/T_w$. Equation (2.16) implies that for a fixed T_w at temperature T, the optical dephasing rate is determined by all perturbers coupled by $C(R)$ with relaxation rates greater than $1/T_w$. In this context, the intrinsic fluctuation rate distribution at temperature T is

$$P_i(R) = \int dE P(E,R) \mathrm{sech}^2(E/2kT). \tag{2.17}$$

Thus, $P_i(R)$ has the identical definition as $P(R)$ in Eq. (3.2a) in Ref. 14; $P_i(R)$ is the energy averaged relaxation-rate distribution of the thermally accessible perturbers. $P_i(R)$ describes the bulk fluctuations of the sample at a given temperature.

The energy distribution function $P(E)$ is often taken as $P(E) \propto E^{\mu}$ with a cutoff at $E = E_{\max} \gg kT$. The exponent μ takes on a value between 0 and 1.[35] The average over the energy distribution has the effect of limiting the integral over the rate R to a maximum value of R, $R_{\max}(2kT)$.[14] Thus, the four-time correlation function in Eq. (2.8) is

$$C(\tau, T_w, \tau) = \exp\left(-\frac{2\pi^2 N \bar{\eta}}{3V} \tau \int_{R_{\min}}^{R_{\max}} dR \; P_i(R) C(R) \times [1 - \exp(-RT_w)] \right). \tag{2.18a}$$

This permits the definition of the coupled distribution of rates, $P_c(R) = P_i(R)C(R)$. In terms of $P_c(R)$ the four time correlation function is

$$C(\tau, T_w, \tau) = \exp\left(-\frac{2\pi^2 N \bar{\eta}}{3V} \tau \int_{R_{\min}}^{R_{\max}} dR \; P_c(R) \times [1 - \exp(-RT_w)] \right). \tag{2.18b}$$

To determine $P_c(R)$, a stimulated echo experiment is performed for a series of different waiting times T_w. T_w is the time between the second and third pulses, and the echo signal is recorded as a function of τ, the delay time between the first and second pulses. The signal decay as a function of τ is proportional to the averaged four point correlation function given in Eq. (2.18b). The directly measurable quantity is the integrated intensity of the echo pulse $I_S(\tau; T_w)$. The echo decay function $I_S(\tau; T_w)$ is proportional to the Fourier transform of the hole spectrum in a hole burning experiment.[12,14] Data from stimulated photon echo experiments and hole burning experiments performed on the same chromophore and solvent yield the same information on the distribution of coupled rates $P_c(R)$, which is determined by the intrinsic distribution of rates $P_i(R)$ and the rate dependent coupling function $C(R)$.

Equations (2.18a) and (2.18b) show the fundamental difference between the theoretical model presented here and that given[13,14] and used[14,29,32,34] previously. Previously, $C(R)$ was taken to be a constant independent of R. It was pulled outside of the integral in Eq. (2.5a). Therefore, the hole burning or stimulated echo experimental observables were considered to be directly related to the intrinsic distribution of rates in the glass. Furthermore, since the coupling was assumed to be independent of R, there was no possibility that $C(R)$ could have a functional form that depended on the chromophore used as a probe in the experiment. In the context of the old theory, any chromophore could be used to map out the intrinsic distribution of rates. Equation (2.18b) shows that the experiment actually measures $P_c(R) = P_i(R)C(R)$. Therefore, the experimental observables yield the distribution of rates modified by the functional form of the strength of the coupling. Since the rate dependent coupling can vary with R in different manners for different chromophore probes, the observed $P_c(R)$ can be chromophore dependent. This is consistent with the experimental observations discussed later.

As can be seen from Eq. (2.18b), the stimulated photon echo signal $I_S(\tau; T_w)$ varies with waiting time T_w as

$$\ln I_s(\tau; T_w) \propto -\int_0^{1/\tau} dR P_c(R)[1 - \exp(-RT_w)]. \tag{2.19}$$

Equation (2.19) does not include populational relaxation, T_1. When the line shape is Lorentzian (the echo decay is exponential), the decay of the echo as τ is scanned is given in terms of the decay constants T_2 (the total dephasing time), T_1 and T_2^* (the pure dephasing time)[21,22]

$$I_s(\tau; T_w) = \exp(-4\tau/T_2), \tag{2.20}$$

with

$$\frac{1}{T_2(T_w)} = \frac{1}{2T_1} + \frac{1}{T_2^*(T_w)}. \tag{2.21}$$

In the frequency domain, the corresponding linewidth, Γ is

$$\Gamma(T_w) = \frac{1}{\pi T_2(T_w)} = \frac{1}{2\pi T_1} + \frac{1}{\pi T_2^*(T_w)}. \tag{2.22}$$

For a chromophore in a glass at sufficiently low temperature, the pure dephasing has two contributions, the homogeneous dephasing, which is T_w independent, and spectral diffusion, which depends on T_w. The homogeneous dephasing is determined by the two pulse photon echo experiment or the three pulse stimulated echo with $T_w = 0$. The spectral diffusion contribution is obtained from either a stimulated echo experiment or a hole-burning experiment. These are conducted as a function of T_w. In the experiments, all of the echo decays are exponential and the spectral holes are Lorentzian. Therefore the data can be discussed using Eqs. (2.18)–(2.22).

The derivative of the logarithm of the echo-decay function [Eq. (2.19)] with respect to T_w measures the increase in the pure dephasing time $T_2^*(T_w)$ with increasing waiting time, i.e., the rate at which spectral diffusion increases the linewidth as T_w increases as

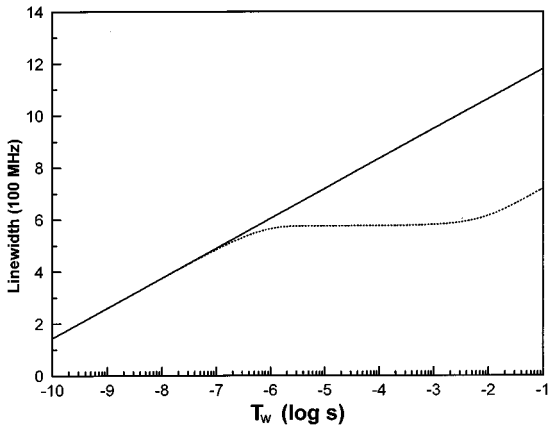

FIG. 1. Linewidth from spectral diffusion vs T_w for two cases. The solid line is obtained with $C(R)=1$, i.e., the coupling of the chromophore to the TLS is independent of the rate, R, of the TLS fluctuation. The dashed line is obtained with $C(R)=0$ in the range $10^2<R\leqslant 10^6$ and one elsewhere. The two curves are calculated for the same intrinsic fluctuation rate distribution, $P_i(R)$. The plateau in the linewidth vs T_w curve occurs in spite of the fact that $P_i(R)\neq 0$. The observable is related to the coupled rate distribution, $P_c(R)$, not $P_i(R)$. Experimental results will only yield $P_i(R)$ when $C(R)$ is a constant for all R, as in the solid line.

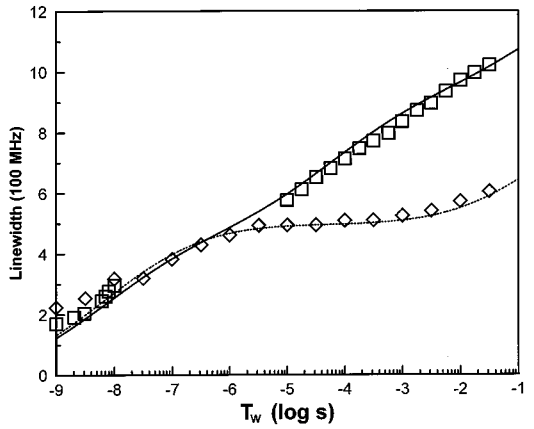

FIG. 2. Data taken on MgP and CV in EtOD with stimulated photon echo and hole burning experiments. Diamonds, linewidths of MgP measured by Meijers and Wiersma with stimulated photon echoes (Ref. 32). Squares with $T_w>10^{-5}$ s, linewidths of CV measured by Littau and Fayer using fast hole burning (Ref. 29). Squares with $T_w<10^{-7}$, linewidths of CV from the stimulated photon echo data presented in Sec. IV. The solid line through the CV data and the dashed line through the MgP data are calculations using the intrinsic fluctuation rate distribution, $P_i(R)$, and coupling functions, $C(R)$, shown in Fig. 3. Both calculated curves are obtained using the same $P_i(R)$. The solid line through the CV data uses $C(R)=1$, i.e., rate independent coupling. The dashed line through the MgP data uses $C(R)$ shown in curve *b* of Fig. 3.

$$\frac{\partial \ln(I_s)}{\partial T_w} \propto -\int dR P_c(R) R \exp(-RT_w)$$

$$= -\int dR P_c^{\ln}(R) \exp(-RT_w). \tag{2.23}$$

The substitute function $P_c^{\ln}(R)$ is the coupled distribution of rates on a $\ln(R)$ scale:

$$P_c^{\ln}(R) d(\ln R) = P_c(R) dR. \tag{2.24}$$

It is seen from Eq. (2.23) that the derivative of the logarithm of the echo signal with respect to T_w is proportional to the Laplace transform of $P_c^{\ln}(R)$.[12,14]

To illustrate the role rate dependent coupling can have on experimental observables, a very simple model is presented prior to considering the experimental data. The intrinsic fluctuation rate distribution is $P_i(R)=1/R$. Two possible coupling functions, $C(R)$, are considered. One is $C(R)=1$ for all R. This is the assumption that has been used in the previous theory and in the analysis of experimental data. The second $C(R)$ is also equal to one except in the range $10^2<R\leqslant 10^6$ where it is zero. Figure 1 shows calculated linewidths vs T_w that are obtained by numerically integrating the Eq. (2.19). The solid line is for the case $C(R)=1$ for all R. Thus, $P_c(R)=P_i(R)$. The dashed line in Fig. 1 is calculated using the $C(R)$ with the zero region. Like the solid line, the dashed line exhibits a constant positive slope where $P_c(R)\neq 0$. However, unlike the previous case, where $C(R)=0$, the corresponding slope is zero, and the increase of the linewidth with T_w plateaus. The plateau in the linewidth vs T_w curve occurs in spite of the fact that $P_i(R)\neq 0$. The observable is related to $P_c(R)$ not $P_i(R)$. Experimental results will only yield $P_i(R)$ when $C(R)$ is a constant for all R, as in the solid line in Fig. 1.

III. EVIDENCE FOR THE RATE DEPENDENT COUPLING

As mentioned in Sec. I, there is experimental evidence that different chromophores in the same glass yield different observed rate distribution functions. These have been interpreted previously as measurements of $P_i(R)$, and no rationale has been given for differences that were observed when different chromophores were used in the same glass. The theory presented earlier, which includes $C(R)$, can be used to rationalize the differences. Fast spectral hole-burning measurements performed by Littau and Fayer[29] on the cationic dye cresyl violet in phase I ethanol-*d* (EtOD) glass at 1.5 K were interpreted as giving $P(R)\propto 1/R$ over the limits 10^1 Hz$<R<10^5$ Hz. However, stimulated photon echo measurements performed by Meijers and Wiersma[30–32] on the neutral chromophore magnesium porphine (MgP) in the same solvent at the same temperature were interpreted as

$$P(R)=\begin{cases} 1/R, & 10^1 \text{ Hz}<R\leqslant 10^3 \text{ Hz} \\ 0, & 10^3 \text{ Hz}<R\leqslant 10^6 \text{ Hz}. \\ 1/R, & 10^6 \text{ Hz}<R<10^9 \text{ Hz} \end{cases} \tag{3.1}$$

These results conflict in the region 10^3 Hz$<R<10^5$ Hz.

Figure 2 displays data taken on MgP and CV in EtOD with stimulated photon echo and hole burning experiments. The diamonds are the linewidths of MgP in EtOD measured

by Meijers and Wiersma with stimulated photon echoes.[32] The squares with $T_w > 10^{-5}$ s are the linewidths of CV in EtOD measured by Littau and Fayer using fast hole burning.[29] The hole burning results are related through a Fourier transform to the stimulated echo results. Hole-burning linewidths are divided by 2 (Ref. 29) to make them directly comparable to linewidths obtained from stimulated echoes. The squares with $T_w < 10^{-7}$ are the linewidths of CV in EtOD from the stimulated photon echo data presented in this paper in Sec. IV. (The calculated curves through the data are discussed later.) The homogeneous linewidth ($T_w = 0$) for MgP is 159 MHz and for CV is 153 MHz. All three experiments were performed in the same solvent, phase I glassy EtOD at 1.5 K. Figure 2 shows the profound difference in the data taken on the two chromophores in the range of rates 10^3 Hz $< R < 10^5$ Hz.

It is possible to replicate the nature of the differences seen in Fig. 2 using the concepts presented in Sec. II. To do this, a heuristic model of the nature of the TLS dynamics and rate dependent coupling is presented. The model will be discussed in terms of physical features of the chromophores and the glassy system, but it is not intended to be presented as a unique, accurate microscopic description.

We will model the distribution of TLS rates as the sum of three log normal distributions. Small and co-workers[37] have argued that observables calculated for a $1/R$ distribution of rates can be well approximated using a sum of log normal distributions. To permit a physical bases for the sum of three distributions and how they might be related to the distribution of coupling strength, $C(R)$, we assign to each of the three distributions an underlying physical mechanism.

A. High-frequency translational TLS

High-frequency TLS arise from translational motions of the molecules forming the glass. The two potential wells of the TLS correspond to two positions on a displacement coordinate with basically no change in orientation. Since EtOD has a permanent electric dipole, translation will result in a change in the dipolar field at the chromophore. The translation will also cause a change in the local strain, and thus, will be felt at the chromophore as a change in the strain dipolar field.

B. Mid-frequency rotational TLS

Mid-frequency TLS arise from orientational motions of the molecules forming the glass. The two potential wells of the TLS correspond to two positions on a rotational coordinate with basically no change in position of the center of mass. Since EtOD has a permanent electric dipole, rotation will result in a change in the dipolar field at the chromophore. It is assumed that rotation in the absence of translation of the center of mass of the molecule does *not* cause a change in the local strain, and thus, will *not* be felt at the chromophore as a change in the strain dipolar field.

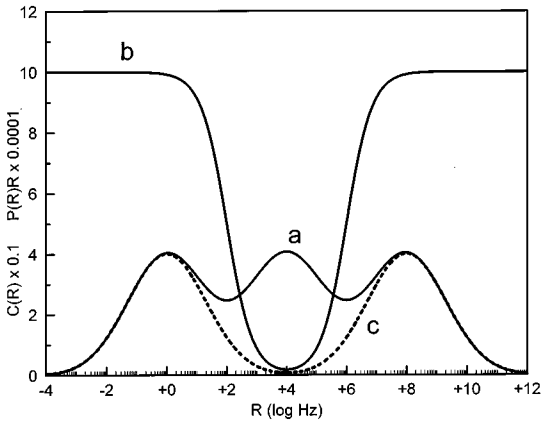

FIG. 3. Curve *a*, the model intrinsic fluctuation rate distribution, $P_i(R)$, which is a sum of three log normal distributions. This $P_i(R)$ is used in the calculations of both the CV and MgP data shown in Fig. 2. Curve *b*, coupling function $C(R)$ used in the calculation of the MgP data shown in Fig. 2. The model coupled rate distribution, $P_c(R) = C(R)P_i(R)$ for MgP is shown in curve *c*. For CV, $C(R) = 1$. Therefore, for CV, curve *a* is both $P_c(R)$ and $P_i(R)$. The difference in $P_c(R)$ for CV and MgP is responsible for the difference in the calculated fits to the data shown in Fig. 2.

C. Low frequency complex aggregate motion TLS

Low-frequency TLS arise from the concerted single step movement of many of the molecules forming the glass. The two potential wells of the TLS correspond to two positions of the aggregate, and involve both changes in the center of mass and the orientation. The translational and rotational motion of the aggregate causes a change in the electric and strain dipolar fields felt at the chromophore.

Each of these three classes of TLS perturbers contribute to the rate distribution $P_i(R)$, peaking at three seperate rates R_f, R_m, and R_s, where f, m, and s correspond to fast, mid-range, and slow rates, respectively. Then the form of the intrinsic rate distribution, $P_i(R)$, the sum of three log normal distributions, is

$$P_i(R) = \frac{\Omega_f}{R} \exp \frac{-[\ln(R/R_f)]^2}{(2\sigma_f^2)} + \frac{\Omega_m}{R} \exp \frac{-[\ln(R/R_m)]^2}{(2\sigma_m^2)} + \frac{\Omega_s}{R} \exp \frac{-[\ln(R/R_s)]^2}{(2\sigma_s^2)}. \tag{3.2}$$

The σ are the standard diviations on a log scale and the Ω are normalization constants. Figure 3 shows a plot of Eq. (3.2) with the parameters $R_f = 10^8$ Hz, $R_m = 10^4$ Hz, $R_s = 10^0$ Hz, $\sigma_f = \sigma_m = \sigma_s = 3.0$, and $\Omega_f = \Omega_m = \Omega_s = 400$. These are the parameters used in the calculations to model the data. $P_i(R)$ is curve *a* in Fig. 3. Note that the horizontal axis is a log

scale. The three distributions overlap substantially. There is no abrupt separation of the time scales for the three different processes.

The form of $C(R)$ for this heuristic model is based on the differences in the properties of the two chromophores. CV is an ionic species with a substantial permanent dipole moment which has a significant change in dipole moment upon excitation into the excited state. The dipole moment difference will couple to the fluctuating electric dipolar field produced by the TLS. CV will also couple to the fluctuating strain dipolar field through the density dependence of the transition energy. In the model, all three types of the TLS, spanning all rates, produce fluctuating electric dipoles. Therefore, we take $C(R)=1$ for all R, and $P_c(R)=P_i(R)$. The coupled distribution is equal to the intrinsic distribution of rates. Then, in Fig. 3, curve a is $P_c(R)$ for CV.

In contrast to CV, MgP is a neutral molecule with no permanent dipole moment or dipole moment change upon excitation. In the model, MgP is assumed to couple to the fluctuating strain dipolar field but not to the electric dipolar field. Since the mid-frequency TLS do not result in fluctuating strain dipoles, MgP will not couple to this portion of $P_i(R)$; $P_c(R)\neq P_i(R)$. The form of $C(R)$ for MgP is

$$C(R)=1-\left(1+\frac{\rho_f \exp\{-[\ln(R/R_f)]^2/(2\sigma_f^2)\}+\rho_s \exp\{-[\ln(R/R_s)]^2/(2\sigma_s^2)\}}{\rho_m \exp\{-[\ln(R/R_m)]^2/(2\sigma_m^2)\}}\right)^{-1}. \tag{3.3}$$

$C(R)$ for MgP is shown in Fig. 3 as curve b. The resulting $P_c(R)=C(R)P_i(R)$ for MgP is shown in Fig. 3 as curve c. The effect of $C(R)$ is to produce a coupled rate distribution for MgP which does not include the mid-range TLS log normal component of the intrinsic rate distribution.

Using Eq. (3.2) and the parameters given below it for $P_i(R)$ along with Eq. (3.3) for the MgP $C(R)$, and performing the linewidth calculation by numerically integrating Eq. (2.19), the curves through the data in Fig. 2 were obtained. The solid line through the CV data uses $P_c(R)=P_i(R)$ given by curve a in Fig. 3. The dashed line through the MgP data uses $P_c(R)$ given by curve c in Fig. 3. The agreement is good for both chromophores except at very short T_w since Eq. (2.19) assumes that $T_w>10\tau$ (see Sec. II A). The important point is that both calculations use the same intrinsic rate distribution, $P_i(R)$. The differences arise because of differences in the rate dependent coupling, $C(R)$, which are brought about by the different physical properties of the chromophores.

The agreement between the calculation based on the simple physical model and the data is good but by no means perfect. It is possible to obtain perfect agreement by using either a more complicated form of $C(R)$ or of $P_i(R)$. In the original discussion of the CV hole burning data,[29] the results were interpreted as arising from $P_i(R)=1/R$ with $C(R)$ implicitly assumed to be equal to a constant. This gives a better fit to the CV data than the three log normal distributions used in the model calculations. The MgP data can be reproduced for a $P_i(R)=1/R$ distribution if an appropriate from of $C(R)$ is used. It is also important to note that it is not necessary to have $C(R)$ be identically zero to obtain results with a plateau. If $C(R)$ becomes small over some range, and the form of $C(R)$ and $P_i(R)$ are appropriate, the MgP data can also be reproduced.

These results demonstrate that rate dependent coupling for different chromophores in the same solvent can drastically alter the observation of spectral diffusion. Had experimental data been available only for the neutral chromophore MgP, it would not be clear whether $C(R)$ or $P_i(R)$ goes to zero in the plateau region. Meijers and Wiersma interpreted their stimulated echo results by assuming that $P_i(R)$ is zero in the plateau region. The CV data and the analysis given above demonstrates that this is not a reasonable interpretation. While it is not possible to give a unique interpretation of the data, a principle can be put forward that states the more dynamics observed, the closer the observation is to reflecting the system properties. Fluctuations that exist can be unobservable if the coupling is zero. Fluctuations that do not exist, cannot be observed. This can be seen clearly in other contexts. Optical hole-burning experiments and other experiments on Pr^{+3} in LaF_3 crystals[10] reveal long time scale spectral diffusion arising from the coupling of the paramagnetic Pr^{+3} ion to the fluctuating magnetic fields produced by F spin flips.[10,14] If Pr^{+3} were to be replaced with a nonparamegnetic species, the coupling to the spin flips and the spectral diffusion would vanish. However, the F spin dynamics would not cease; they would just be unobservable in a spectral diffusion experiment.

The experiments on MgP and CV point out the usefulness of performing spectral diffusion measurements in glasses on more than on chromophore. The fact that MgP has a range of R for which $C(R)$ is zero while CV does not suggests that the underlying TLS are not of a single type. It was mentioned earlier, that it is possible to fit the MgP data with $P_i(R)=1/R$ and an appropriate form of $C(R)$. However, the results suggest that there cannot be a single nature of TLS that gives rise to the distribution. If all TLS involve the same basic physical motions, but with a distribution of rates arising from a distribution of tunneling parameters, it is unreasonable to postulate that over some range of R, $C(R)=0$. Therefore, the plateau seen in the MgP data that is absent in the CV data strongly suggests that the TLS are divided into different classes in manner akin to the simple heuristic model presented earlier.

IV. ADDITIONAL EVIDENCE OF RATE DEPENDENT COUPLING FROM SHORT T_W EXPERIMENTS

The data displayed in Fig. 2 shows a dramatic difference between the spectral diffusion observed with the two chromophores, CV and MgP, in the time range 10^{-3}–10^{-5} s. Fast time scale three pulse stimulated photon echo experiments were performed on CV and zinc meso-tetra phenyl porphine (ZnTPP) in EtOD at 1.5 K to determine if there are also differences in $C(R)$ in the time range 0 ns$\leqslant T_w \leqslant$20 ns. ZnTPP was used rather than MgP because it is more readily available, and it is virtually identical in its properties to MgP and zinc porphine (ZnP), also studied by Meijers and Wiersma.[32] ZnTPP, MgP, and ZnP should couple to the TLS in the same manner.

A. Experimental methods

The picosecond laser system used in these experiments has been described in detail previously.[20] It is an amplified sync-pumped dye laser producing tunable 1.5 μJ near transform limited 4 ps pulses at repetition rate of 1 KHz (although the repetition rate was lowered to 10 Hz for ZnTPP). While ZnTTP does not undergo permanent hole burning, CV does. The discussion in this section will focus on new methods that have been developed to perform echo experiments on samples that undergo extensive hole burning.

Cresyl violet (CV, Exciton) and zinc meso-tetra phenyl porphine (ZnTPP, Porphyrin products) were used without further purification. Solutions of CV and ZnTPP were prepared in deuterated ethanol (C_2H_5OD, EtOD) so that the absorbance at the excitation frequency was about 0.8 in a 1 mm thick cuvette. This corresponds to concentrations of 5×10^{-4}–1×10^{-3} M. The excitation wavelength of CV was 620 nm, and ZnTPP was 595 nm. The solutions were sealed in special cuvettes under dry nitrogen. It was found that the thermal conductivity of the cuvette glass was poor enough that if superfluid liquid helium was not allowed to permeate the EtOD glass, the EtOD glass would rise in temperature when exposed to the laser beams. The sealed cuvettes were fitted with a glass arm which could be broken off the cuvette by pushing the sample rod down against the floor of the cryostat, allowing the superfluid helium to rush in and directly cool the glass inside.

To perform the stimulated echoes, the single ps pulse was split into three pulses and sent down delay lines to provide the necessary τ and T_w delays. One mirror in the path of pulse two was mounted on an oscillating piezo-electric transducer. This made a very small time dependent variation in path length (phase), preventing the generation of an accumulated echo signal.[6,34] Stimulated photon echo decay curves were taken by measuring the integrated intensity of the echo vs τ at a fixed a T_w. The maximum possible delay for T_w was 20 ns. The crossed beams in the sample had a diameter ($\pi\omega_0$) of approximately 200 μM.

While the signal from a stimulated echo experiment is in principle background free, the windows from the cryostat and sample surface generate scatter comparable to the maximum intensity of the echo. Furthermore, the scatter was not time independent. As the cresyl violet hole burned, its optical density decreased, and the amount of scattered light increased. To correct the artifact of a baseline varying with the time dependent amount of scatter, a differential amplification scheme was employed. A mask with two apertures was placed between the sample and two matched photodiode detectors. The first (signal) aperture was placed in the phase-matched direction for the stimulated echo. The transmitted echo and scatter were focused onto the first detector. The second (scatter) aperture was placed close to the signal so that the scatter was well correlated to that seen by the signal photodiode, but no signal passed through it to the scatter photodiode. The signal and scatter photodiodes were connected to matched transimpedance amplifiers whose outputs were connected to a differential amplifier. The detectors were nulled by making pulse 1 come after pulse 2 so that there was no echo but only scatter passing through the apertures. A variable neutral density wheel placed in one of the beams was adjusted until the differential amplifier output was zero. The output of the differential amplifier represented only the echo signal with the contribution from scattered light removed.

The τ delay line was run quickly over the scan range of several nanoseconds (usually within 30–40 s). This minimized the artifacts associated with any permanent holeburning, although the cresyl violet still burned sufficiently in this time to require further correction. The PHB results in a substantial decrease in the signal intensity over the time the sample is exposed to the laser pulses. Several techniques were used to minimize this artifact. Laser-induced hole filling was performed before each scan.[34,38] This allowed the same spot on the sample to be used repeatedly. A small portion of the 532 nm doubled cw mode-locked beam (100 mW) was focused onto the hole burned location on the sample for 5 s. The sample was then allowed to equilibrate for 45 s (longer than the length of a typical scan) so that the stimulated photon echo was performed on a glass which was in thermal equilibrium. Although this allowed the same spot to be reused, the hole burning still occurred rapidly enough during a single scan to alter the decay. To correct this artifact, a ''hole-burning curve'' was taken by collecting the photon echo signal at a constant time τ (close to $\tau=0$) vs irradiation time. Any baseline offset was removed from both the actual data and the hole-burning curves and the data were divided by the hole-burning curve. Data were also taken by scanning the delay line in ''reverse'', i.e., from long to short τ, which reverses the apparent hole-burning artifact. These ''reverse'' curves were also divided by the hole-burning curves and the photon echo decays from the ''forward'' and ''reverse'' scans were found to be identical, indicating that the hole burning artifact had been removed.

ZnTPP did not exhibit any noticeable permanent hole burning in EtOD. However, ZnTPP has a very large triplet yield (>90%) and a long triplet lifetime (30 ms). If the laser is operated at 1 KHz, the signal is lost due to population accumulation in the triplet state. Therefore, a repetition rate of 10 Hz was used for the ZnTPP experiments.

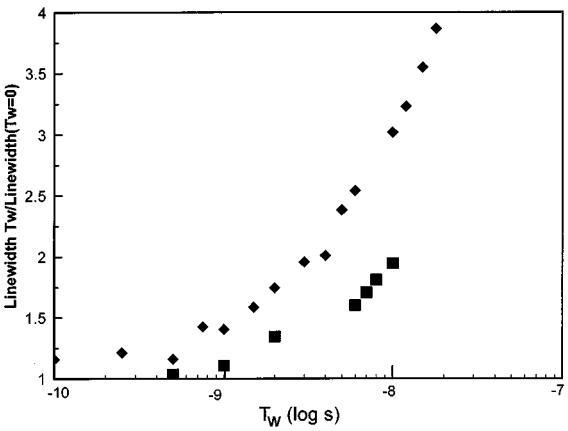

FIG. 4. Stimulated photon echo data for cresyl violet and zinc meso-tetra phenyl porphine (ZnTPP) in EtOD glass at 1.5 K showing fast time scale spectral diffusion. The experimentally measured linewidths, $\Gamma^*_{\rm hom}(T_w)$, were divided by the homogeneous linewidth, $\Gamma^*_{\rm hom}(T_w=0)$, and plotted vs $\log(T_w)$. The diamonds are the linewidth ratios for ZnTPP. The squares are the linewidth ratios for CV. The division removes the magnitude of the coupling to the TLS. If the coupling function, $C(R)$, is independent of R, the data from the two chromophores should be identical. The difference in the data shows that $C(R)$ depends on rate for fast rates like it does for slower rates as manifested in the data and calculations of Fig. 2.

B. Experimental results

Both the CV and ZnTPP stimulated photon echo decays were single exponentials. Since the decays were exponential, the lifetime could be removed using the relation in Eq. (2.21) to yield the pure dephasing time as a function of T_w. For CV in EtOD at 1.5 K, $T_1=5.5$ ns. For ZnTPP in EtOD at 1.5 K, $T_1=2.1$ ns.[12,31] The homogeneous linewidth ($T_w=0$) for ZnTPP is 170 MHz and for CV was 153 MHz. In Fig. 4 the data are plotted as the ratio of the T_w dependent linewidth, $\Gamma^*_{\rm hom}(T_w)$, divided by the homogeneous linewidth ($T_w=0$) $\Gamma^*_{\rm hom}(T_w=0)$ vs $\log(T_w)$. If the T_w dependent linewidths depend only on $P_i(R)$, i.e., $C(R)$ is a constant for the range of R covered by the range of T_w, then dividing by the homogeneous linewidth divides out the coupling constant. The result should be linewidths that increase with T_w but are independent of the chromophore. In Fig. 4, the dark squares are the linewidth ratios for ZnTPP, and the light squares are the linewidth ratios for CV.

As is evident from the data, the T_w dependent linewidths for the two chromophores are not identical. ZnTPP exhibits noticeable spectral diffusion at $T_w=1$ ns. In contrast, the linewidth of CV does not increase substantially until $T_w=10$ ns. These results indicate that even for fast rates, $C(R)$ is not constant. Like the long time scale data discussed in Sec. III, it suggests distinct subsets of TLS, operating on the same time scale, but having features that cause then to couple differently to the nonpolar ZnTPP than to the polar CV. It is important to emphasize, that if the difference arises only because of a different magnitude of the coupling of the two chromophores to the TLS, the division of the data sets by the corresponding homogeneous linewidths would make the data shown in Fig. 4 identical. The fact that the spectral diffusion in the ZnTPP system turns on at shorter time suggests that there are TLS with large rates that couple well to ZnTPP but weakly or not at all to CV. Thus, even on a fast time scale, $P_c(R)$ is not necessarily equal to $P_i(R)$.

V. CONCLUDING REMARKS

By extending the sudden jump TLS model of electronic dephasing in glasses to include the possibility of rate dependent coupling of the electronic states to the TLS, the apparent contradiction of two different chromophores showing substantially different spectral diffusion has been reconciled. The fundamental point is that the observation of spectral diffusion by experiments such as stimulated echoes or hole burning does not measure directly the intrinsic fluctuation rate distribution of a glass or other material. The spectral diffusion of a probe chromophore reflects the true distribution of fluctuation rates only if all of the dynamical processes that give rise to the fluctuations couple to the states of the probe equally. The spectral diffusion experimental observable reflects the coupled distribution of rates, which is related to the intrinsic distribution through $P_c(R)=C(R)P_i(R)$, where $C(R)$ is the rate dependent coupling strength. If $C(R)$ has structure, then the spectral diffusion observable will not yield the intrinsic rate distribution. This fact was seen dramatically in the comparison of the data for MgP and CV. The MgP data has a plateau spanning three decades of R while the CV data does not.

To illustrate the ideas of rate dependent coupling in a concrete manner, a heuristic model was presented. In this model, differences in the physical properties of the two chromophores were used to understand possible differences in $C(R)$. MgP, neutral with no dipole moment, will couple to stain dipoles. CV, changed and polar, will also couple to electric dipoles. The full intrinsic TLS fluctuation rate distribution was modeled as being composed of the sum of three log normal distributions, each spanning a different, but overlapping, range of rates. It was assumed that the TLS corresponding to the mid-range log normal distribution of rates caused fluctuating electric dipoles but not strain dipoles. This model, while not unique, was sufficient to reproduced the MgP data with its plateau in spectral diffusion and the CV data, which does not have a plateau. Thus, with rate dependent coupling, it is possible for the same intrinsic rate distribution to give rise to very different spectral diffusion observables.

ACKNOWLEDGMENT

This work was supported by the National Science Foundation, Contract No. DMR93-22504.

[1] *Amorphous Solids: Low Temperature Properties*, edited by W. A. Phillips (Springer, New York, 1981).
[2] R. M. Macfarlane and R. M. Shelby, J. Lumin. **36**, 179 (1987).
[3] *Persistant Spectral Hole-Burning: Science and Applications*, edited by W. E. Moerner (Springer-Verlag, Berlin, 1988).
[4] N. A. Kurnit, I. D. Abella, and S. R. Hartmann, Phys. Rev. Lett. **13**, 567 (1964).
[5] M. J. Weber, in *Laser Spectroscopy of Solids*, edited by W. M. Yen and P. M. Selzer (Springer, New York, 1981).
[6] W. H. Hesselink and D. A. Wiersma, Phys. Rev. Lett. **43**, 1991 (1979).

[7] R. Beach and S. R. Hartmann, Phys. Rev. Lett. **53**, 663 (1984).
[8] M. D. Levenson, *Introduction to Nonlinear Laser Spectroscopy* (Academic, New York, 1982).
[9] A. Szabo, Phys. Rev. B **11**, 4512 (1975).
[10] R. M. Shelby and R. M. Mcfarlane, J. Lumin. **31&32**, 839 (1984).
[11] C. A. Walsh, M. Berg, L. R. Narasimhan, and M. D. Fayer, J. Chem. Phys. **86**, 77 (1987).
[12] M. Berg, C. A. Walsh, L. R. Narasimhan, K. A. Littau, and M. D. Fayer, J. Chem. Phys. **88**, 1564 (1988).
[13] Y. S. Bai and M. D. Fayer, Chem. Phys. **128**, 135 (1988).
[14] Y. S. Bai and M. D. Fayer, Phys. Rev. B **39**, 11066 (1989).
[15] D. E. McCumber and M. D. Sturge, J. Appl. Phys. **34**, 1682 (1963).
[16] J. L. Skinner and D. Hsu, Adv. Phys. Chem. **65**, 1 (1986).
[17] M. T. Loponen, R. C. Dynes, V. Narayanamurti, and J. P. Garno, Phys. Rev. Lett. **45**, 457 (1980).
[18] M. Meissner and K. Spitzman, Phys. Rev. Lett. **46**, 265 (1981).
[19] M. S. Love and A. C. Anderson, J. Low Temp. Phys. **84**, 19 (1991).
[20] L. R. Narasimhan, K. A. Littau, D. W. Pack, Y. S. Bai, A. Elschner, and M. D. Fayer, Chem. Rev. **90**, 439 (1990), and references therein.
[21] P. Hu and S. R. Hartmann, Phys. Rev. B **9**, 1 (1974).
[22] P. Hu and L. R. Walker, Phys. Rev. B **18**, 1300 (1978).
[23] D. L. Huber, M. M. Broer, and B. Golding, Phys. Rev. Lett. **52**, 2281 (1984).
[24] S. Hunklinger and M. Schmidt, Z. Phys. B **54**, 93 (1984).
[25] P. W. Anderson, B. I. Halperin, and C. M. Varma, Philos. Mag. **25**, 1 (1972).
[26] W. A. Phillips, J. Low Temp. Phys. **7**, 351 (1972).
[27] W. O. Putikka and D. L. Huber, Phys. Rev. B **36**, 3436 (1987).
[28] K. K. Rebane and A. A. Gorokhovskii, J. Lumin. **36**, 3436 (1987).
[29] K. A. Littau, M. A. Dugan, S. Chen, and M. D. Fayer, J. Chem. Phys. **96**, 3484 (1992).
[30] H. C. Meijers and D. A. Wiersma, Phys. Rev. Lett. **68**, 381 (1992).
[31] H. C. Meijers and D. A. Wiersma, Chem. Phys. Lett. **181**, 312 (1991).
[32] H. C. Meijers and D. A. Wiersma, J. Chem. Phys. **101**, 6927 (1994).
[33] R. F. Loring and S. Mukamel, Chem. Phys. Lett. **114**, 426 (1985).
[34] L. R. Narasimhan, Y. S. Bai, M. A. Dugan, and M. D. Fayer, Chem. Phys. Lett. **176**, 335 (1991).
[35] M. J. Weber, J. Lumin. **36** (1987).
[36] J. L. Black and B. I. Halperin, Phys. Rev. B **16**, 2879 (1977).
[37] R. Jankowiak and G. J. Small, Phys. Rev. B **47**, 805 (1993).
[38] A. Rebane and D. Haarer, Chem. Phys. Lett. **70**, 478 (1989).